Investigating cell–material interactions by monitoring and analysing cell migration

J.-P. KAISER, A. BRUININK*
MaTisMed, Biocompatible Materials, Swiss Federal Laboratories for Material Testing and Research (EMPA), Lerchenfeldstrasse 5, CH-9014 St Gallen, Switzerland
E-mail: arie.bruinink@empa.ch

Cell–material interactions can on one hand be characterised by assessing the functional state and or shape of the cells at one or different discrete periods of time, on the other hand by observing cell migration and spreading behaviour. The object of this study was to investigate the migration behaviour of fluorescently labelled cells, and to evaluate the software analysing this migration. In the present study, the behaviour of fibroblasts cells on differently structured surfaces was taken as example. In the first step, the influence of seven different lipophilic dyes (DiI, DiO, DiA, DiD, DiR, PKH2 and PKH26) on cell performance was determined taking biochemical parameters as indices. In the second step, the fluorescence characteristics of these dyes were compared regarding their applicability. In the third step, migration behaviour of DiI-labelled fibroblastic cells on plane and grooved surfaces were monitored and analysed using specific software.

Our data suggest that most of the dyes have optimal characteristics for studying cell – cell interactions. Cell migration behaviour regarding migration direction and cell spreading was different on plane and grooved surfaces. It could be shown that computer-based image analysis represents a practical, quick and objective tool to quantify exactly cell migration behaviour.

Introduction

After implantation beside the release of implant constituents the surface plays a determining role in the implant acceptance and integration in the biological environment. The surface is characterised by its chemical and structural properties as well as by the patterning thereof. Knowledge on which the critical features for the cell reactions are still very sparse and the mechanism of cell–surface interaction is so far not understood. Of the implant point of view an optimal cell–surface interaction results in the colonisation of the implant surface by the correct cell types and is among others determined by attachment and migration of latter cells. Cell migration plays a key role not only in normal physiological processes, such as embryogenesis and morphogenesis, but also in healing processes [1]. The observation and monitoring of the cell shape and migration combined with its detailed analysis may be of key importance in order to understand the mechanisms behind cell migration and which key features of the substratum are essential for its behaviour [2]. So far, few studies have been published on cell migration including cell shape on topographically modified surfaces [3].

In most cases only one aspect was investigated or the analysis was extremely time consuming [4–8]. The disadvantage of the methods described by Cox *et al*. [4] was that cell spreading was assessed after fixation of the samples at a time interval of 10 min and not continuously on the same sample and cells. A similar approach was chosen by Wojciak-Stothard *et al*. [5] and Chehroudi and his team [6] studying the spreading, elongation and orientation of cells on multiple grooved substrata. The microfilaments, microtubules and the focal contact components were also fixed prior, stained and microscopically analysed. Lo *et al*. [7] recorded cell migration by phase contrast and fluorescence microscopy. The migration speeds of individual cells were determined with time-lapse images recorded over a period of 60 min. The position of the centre of the nucleus was measured at 15 min intervals with custom software. The migrated distances of the cells between two pictures were used to determine the mean migration velocity. With this method only one location was monitored at a time and the system was not automised. Curtis *et al*. [8] measured the rate of movement of non-neural cells by time-lapse recording under phase contrast illumination using a video camera and S-VHS recorder. The recordings had been analysed by displaying them on a monitor, frame by frame. The centre of the nuclei of each cell was marked one by one. The migration distance was determined on the monitor screen by measuring the differences in cell centre location between two frames.

*Author to whom all correspondence should be addressed.

The goal of the present study was to develop optimal tools for long-term monitoring of substratum-induced cell behaviour, migration and cell shape of several cell types at various locations on the same sample. To compare vital fluorescent dyes regarding their applicability for long-term observations, seven different dyes were tested. Of each dye the maximal labelling intensity, toxicity and bleaching behaviour was assessed. Furthermore, software to analyse migration, cell shape and velocity was optimised.

Materials and methods

Materials and cultures

In the present study seven different vital dyes, DiI, DiO, DiA, DiD, DiR (all of Molecular Probes, Juro, Luzern, Switzerland), PKH2 and PKH26 (both of Sigma, Fluka Chemie GmbH, Buchs, Switzerland) were compared. Cells of the fibroblastic cell line 3T3 of passage 20–35 were cultured in Dulbecco's Modified Eagle's Medium (DMEM) containing 10% heat-inactivated foetal calf serum (Life Technologies, Basel, Switzerland) and 1% PSN (Life Technologies, Basel, Switzerland) under cell culture conditions (5% CO_2/95% air, 95% humidity and 37 °C). Surfaces tested were PVD titanium coated silicon waver. These wavers were unstructured or contained grooves with 9.8 µm spacing and 1.1 µm depth.

Toxicity of the vital dyes, stain intensity and bleaching characteristics

The central 60 wells of 96 well plates (VWR, Dietikon, Switzerland) were inoculated with 3T3 cells (200 µl cell suspension/well, 15 000 cells/ml) and kept for 24 h before use. The surrounding wells containing medium without cells were used as blanks. To label cells and to test dye toxicity 16 µl ethanol containing no dye or different concentrations of the dyes were added to the cultures. Maximal concentrations tested were 2.5 mg dye per ml in case of DiI, DiO, DiA, DiD, DiR as recommended by Honig and Hume [9] and for PKH2; 2.5×10^{-6} M; PKH26; 5×10^{-6} M as recommended by Horan *et al*. [10]. In addition, five dilutions (0.5, 0.25, 0.125, 0.0625 and $0 \times$) were tested. At higher concentrations difficulties arised to keep the fluorochrome in solution. After an incubation period of 15 min under cell culture conditions, the dye-containing medium was removed. Cultures were washed for three times with 200 µl fresh medium without ethanol and dye. The cultures were cultured with 200 µl medium without dye and ethanol for another seven days at 37 °C. At the end of the culture period, cell number taking DNA content as an index was assessed. For this culture medium was replaced by distilled water (100 µl/well). After 15 min incubation at room temperature 100 µl Hoechst reagent solution (Hoechst 33258 reagent) was added to each well. After 1 h of gyratory shaking in the dark the fluorescence was measured (excitation 360 nm, emission 460 nm). In addition to cell protein, as index for total cell mass, neutral red uptake as index for lysomal activity and measure of cell viability, and the conversion of MTT (3-(4,5-dimethylthiazol-2-yl)-2,5-diphenyltetrazolium bromide) towards the MTT-formazan as index of cell activity was assessed according to Bruinink [11].

Stain intensity and fluorochrome and bleaching characteristics

PKH2 and PKH26, had exactly the same absorption and similar emission spectra as DiO (PKH2) and DiI (PKH26). Because of this only the toxicity of these two vital dyes was determined and were not included in the other tests. Vital dye-stained cells were exposed for up to 60 min to excitation light from a HBO mercury short arc lamp (100 W) (Osram, München, Germany). Each 5 min a laser-scanned picture was taken and the fluorescence intensities of the different dyes were thereafter compared.

In a multicolour examination, three batches of 3T3 fibroblast cells were stained with one of the three lipophilic dyes (DiO, DiI and DiD) prior to mixing the cells. The cell mixture was plated on a cell culture dish. Each dye was activated by separate wavelength. For the different dyes the following laser and excitation and emission wavelength were used: (a) DiO: argon laser (ex. 488 nm; em. BP 505–530 nm), (b) DiI: helium/neon laser (ex. 543 nm; em. LP 560 nm) and (c) DiD: helium/neon laser (ex. 633 nm; em. LP 650 nm). All three dyes could be activated at the same time by the appropriate excitation wavelengths.

Only the combination DiO, DiI and DiD was tested because of the following reasons. Among the seven tested dyes, the dyes DiO, DiI and DiD had the advantage that they have a relatively narrow absorption and fluorescence emission maxima. The absorption and fluorescence maxima of these three dyes were quite well-separated although the fluorescence emission maxima were quite close to the emission maxima (DiO 484 nm/501 nm, DiI 549 nm/565 nm, DiD 644 nm/665 nm). Therefore, it is possible to combine these three dyes for a three-colour labelling since the crosstalk at optimal settings is negligible. In contrast, the absorption and emission spectra of DiA is very broad (excitation 400–530 nm, emission 500–700 nm) and in the range of DiO and DiI. Therefore, it cannot be combined with the latter two dyes. DiR had an absorption maximum at 750 nm and fluorescence maxima at 780 nm. The dye was activated with a helium/neon laser with a wavelength of 633 nm. That means that DiD and DiR were activated with the same excitation wavelength and for the detection of the emitted fluorescence the same optical filters need to be used. Therefore, the combination DiD and DiR is not suitable for multiple fluorescence studies.

Cell migration analysis

Fluorescent vital dye (DiI) labelled fibroblastic 3T3 cells were seeded on plane and grooved sample surfaces. After an incubation period of 15 h at culture conditions enabling attachment and spreading of cells non-adherent cells were removed by washing with culture medium. Thereafter the

samples were transferred into a flow chamber with an inner diameter of 19 mm designed in a way that cells could be kept under cell culture conditions for prolonged periods of time. The chamber contained a cover glass lid, which allowed the observation of the cells.

The temperature was controlled by a thermostat, which was placed nearby the incubation chamber. This thermostat controlled a heating device so that a constant incubation temperature could be maintained. During the experiment no fluid flowed through the chamber. The migration of the cells was monitored by using a Zeiss Axioplan two microscope with a LSM 510 scanning module. Appropriate filters and objective (Zeiss LD-Achroplan 20 × 0.4 corr.) were used. For the observation of the cell migration the Zeiss LSM software Release 2.8 (12/2000) was used. During two days for each 15 min a picture was taken from several previously selected areas of interest (maximal about 45 positions). From the obtained pictures the migration pathway (trajectory), cell shape, cell orientation, migration direction and migration velocity of each cell were estimated by special image analysis software developed by Visiometrics (Konstanz, D) that was adapted according to our needs. Data were further analysed using MS Excel-macros.

The software analysed the cell shape and cell position of each picture. The cell shape is expressed in the ratio between the longest cell diameter and perpendicular to the sum of the longest distance of the outer cell membrane on the left and on the right towards this line. The orientation of the cell was defined as the angle between the *x*-axis of a previously graticule and the line of the longest cell diameter. The maximal possible angle range is by that between 0° and 180°. The cell migration is expressed as cell trajectory. A trajectory is defined as the connection of cell locations at the subsequent different time points at which a picture of the culture was taken. The trajectory is therefore a set of connected lines. Each line on itself can be seen as migration vector with a starting and an end location, a length and an orientation angle relative to a previous by defined graticule. The latter angle has in this case a maximal range between 0° and 360°. After the measurements all data are combined. Regarding angles and migration distances discrete ranges are defined and the number of occurrences at each range are counted. Finally, distribution histograms are obtained.

Results and discussion

The influence of seven different lipophilic fluorescent vital dyes on cell performance in the absence and presence of light has been tested. The applicability of these dyes for long-term cell monitoring was assessed and a computer-assisted image analysing systems for cell migrations analysis was evaluated by using one of the dyes. For this the cell behaviour of vital dye-labelled 3T3 fibroblasts was compared microscopically and by computer analysis.

Effects of vital dye labelling on cell performance

In the absence of light none of the investigated lipophilic dyes affected cell proliferation, cell mass, viability and activity significantly at the concentrations measured. The data for DiI are shown in Fig. 1. These observations are in accordance with the findings of Honig and Hume [9], who showed that the performance of fluorescent carbocyanine dye-labelled neurons was not affected by this labelling.

Under the conditions used for migration monitoring, i.e. taking a picture every 15 min, even after an observation period of several days, during which several hundred pictures had been taken and cell proliferation occurred, the cells still showed a very intensive fluorescence. In addition, cell migration at the beginning of the observation period and at the end was comparable. Therefore, we conclude that the system is suitable for migration and cell observation studies over a time period of several days.

Comparison of dye characteristics

Regarding bleaching characteristics it could be shown that all five dyes (DiO, DiI, DiD, DiA and DiR) were quite photo stable. DiR was the weakest of all five tested dyes. DiR and DiA started to fade after 10 min of exposure to the excitation light. DiO was slightly more stable. DiO started bleaching after 15 min of exposure to the excitation light. DiD and DiI showed the highest photo stability among all the five tested dyes. These two dyes started to fade after 30 min of continuous exposure to the excitation light.

In one experiment three samples of 3T3 fibroblast cells

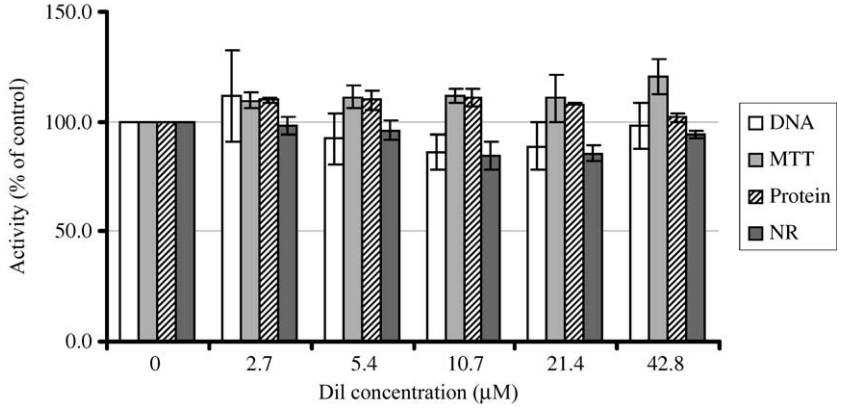

Figure 1 Effects of DiI on cell performance uptake seven days after labelling taking total cell culture DNA, conversion of MTT, cell protein and neutral red uptake (NR) as indices.

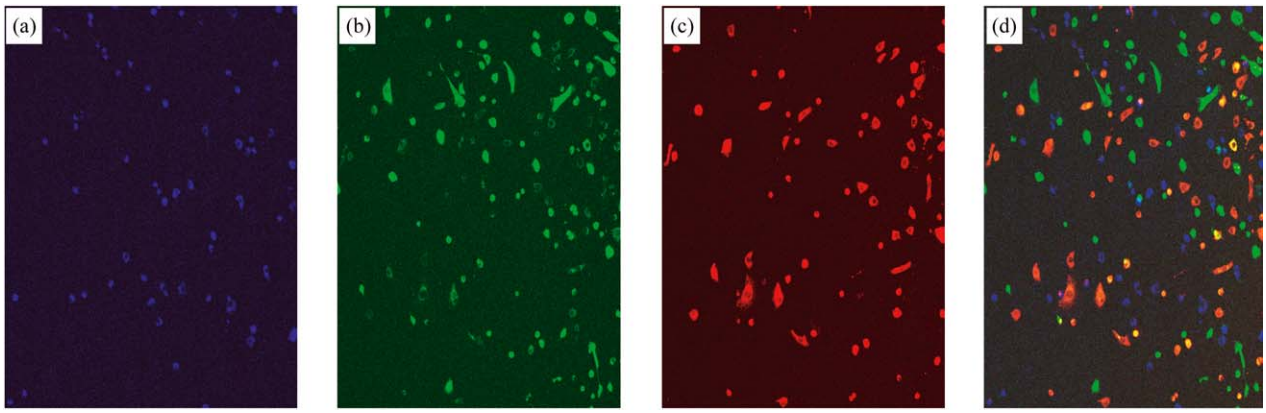

Figure 2 Triple-colour staining. 3T3 fibroblast cells. Cells were labelled with DiO, DiI or DiD and thereafter mixed. (a)–(c) The three dyes were individually excited by their appropriate but different wavelength, (d) all three dyes were excited at the same time.

were stained with three lipophilic dyes (DiO, DiI and DiD) separately, and thereafter mixed in order to visualise the possibility to investigate cell–cell interactions of different populations of cells on non-transparent surfaces. Fig. 2 shows a picture series of this triple-stained cell culture. In Fig. 2(a)–(c) each dye had been activated by its appropriate wavelength. In Fig. 2(d) all three dyes were activated at the same time. This series demonstrate that the crosstalk of these dyes is low. By exciting DiI by a wavelength of 543 nm and using a long path filter > 560 nm for detection of the fluorescence emission, DiD was also slightly activated and showed low fluorescence under these conditions.

Effects of surface structure on cell shape and migration

In our study, the fibroblasts showed a typical ''fibroblastic'' shape without any orientation on plane surfaces (Fig. 3(a)). However, on the grooved surface cells were elongated parallel to the grooves (Fig. 3(b)). These observations were in line with the observations of others. For instance, Brunette [12] demonstrated that cells on structured surfaces were less flattened than cells on plane surfaces. The team of Den Braber [13] reported that dermal fibroblast cells had an elongate shape and aligned parallel to the grooves, when the grooves were narrow. Similar observations have been made by Chehroudi *et al*. [6], who studied the behaviour of epithelial cells on structured surfaces. On smooth surfaces epithelial cells were randomly oriented, whereas on grooved surfaces epithelial cells were oriented along the long axis of the grooves.

Cells on plane and grooved surfaces were migrating, continuously changing their direction. On the plane surface the migration was random with no preferred direction. The migration on the grooved surfaces was mainly bidirectional along the grooves, sometimes the cells trespassed the grooves. These cells exhibited on that moment again the typical fibroblastic shape instead of the elongated cell shape. These observations on differences in cell behaviour on plane and grooved surfaces are in good agreement with the studies of Curtis and Clark [14] and Curtis and Wilkinson [3]. They also observed that certain cell types react very sensitive to specific ranges of size of topography. The reactions to topography included cell orientation, changes in cell migration, cell adhesion and cell shape.

In line with the visual interpretations computer-assisted image analysis of the cell shape revealed that

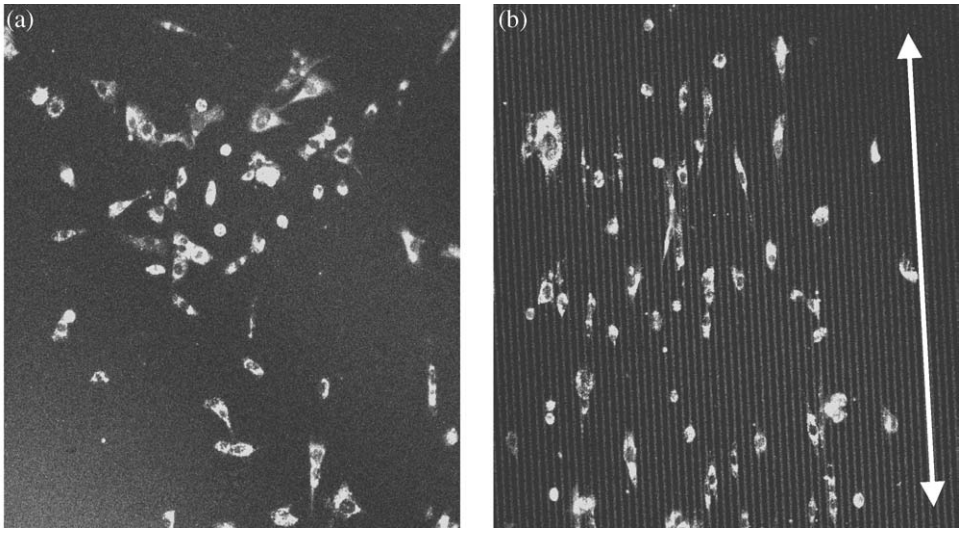

Figure 3 Trajectories of cells kept on a plane (a) and grooved surface (b). On plane surfaces (a) cells were randomly orientated, whereas on grooved surfaces (b) (9.8 μm width, 1.1 μm depth) the cells were orientated along the axes of the grooves. The double arrow represents the groove orientation.

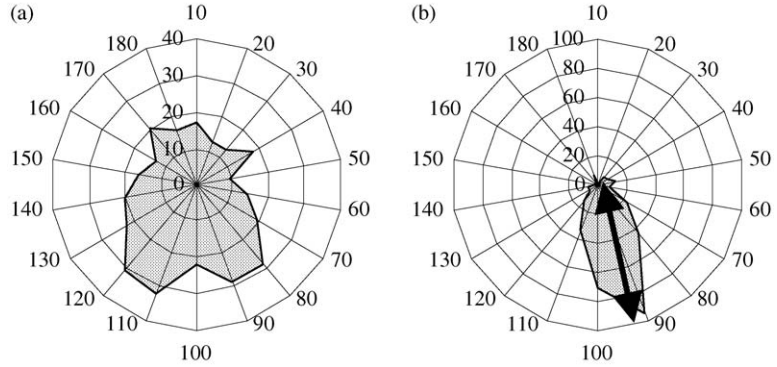

Figure 4 Effects of surface structure on cell orientation (a) plane and (b) grooved surface. The possible range of 0–180° was subdivided into 18 ranges of 10°. Each angle value was allocated to one of these ranges and the frequencies were determined. In both figures the frequency dot are placed in the centre of the range and connected with the adjoining frequency dots, i.e. value shown at 90° means the frequency of orientations between 85° and 95°. The double arrow in the right figure represents the orientation of the grooves.

the cells on the non-structured, plane surfaces were orientated in all directions, with a slight preference to the angels between 80° and 120° (Fig. 4(a)). On grooved surfaces an angle of the long axes of the cells near 90°, i.e. parallel to the grooves was found. Around 61% of the cells had an orientation within the range of 80°–100° and 78% of the cells were orientated within the range of 70°–110° (Fig. 4(b)).

In line to the time-lapse recording the computer analysis revealed that cell migration was strongly determined by surface topography. The covered trails (trajectories) of the cells on the plane and structured surface had been drawn (Fig. 5). The covered trails of the cells on the plane surface were random. The cells changed permanently their directions. The angles of the trajectories were evenly distributed over the whole range between 0° and 360° (Fig. 5(a)). Cell migrations on grooved surfaces were oriented along the axes of the grooves (Fig. 5(b)). The angles of the trajectories on grooved surfaces were quite well orientated in the

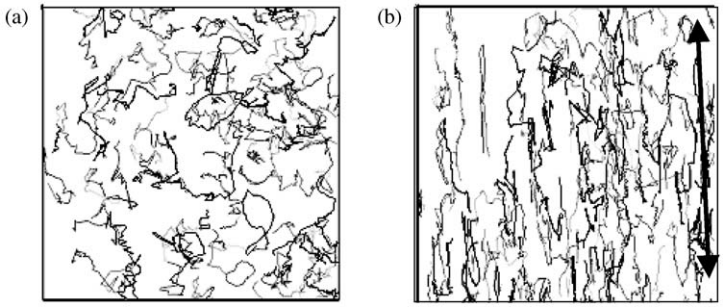

Figure 5 The covered trails (trajectories) of the cells during the observation period of two days. (a) The trajectories of the single cells are recognised by different colour of the trajectories. The migration of the cells on grooved surfaces (b) was oriented in vertical direction along the axes of the grooves. The double arrow represents the orientation of the grooves.

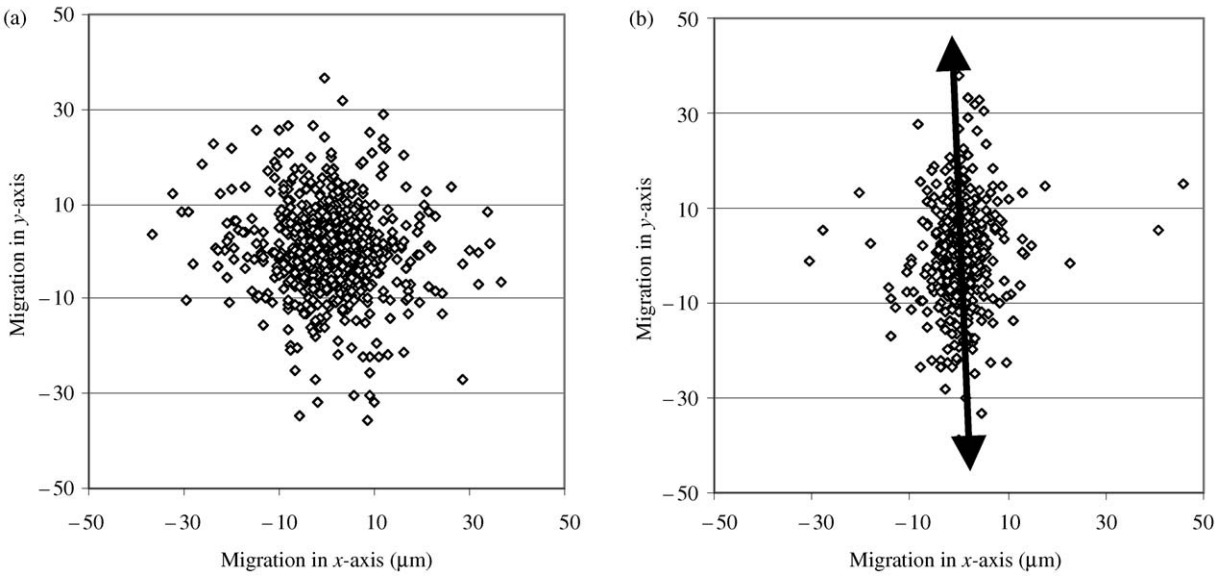

Figure 6 Correlation between migration direction and migration angle (a) plane and (b) grooved surface. Each dot represents the migration vector of one cell between two subsequent pictures. The double arrow in the right figure represents the orientation of the grooves.

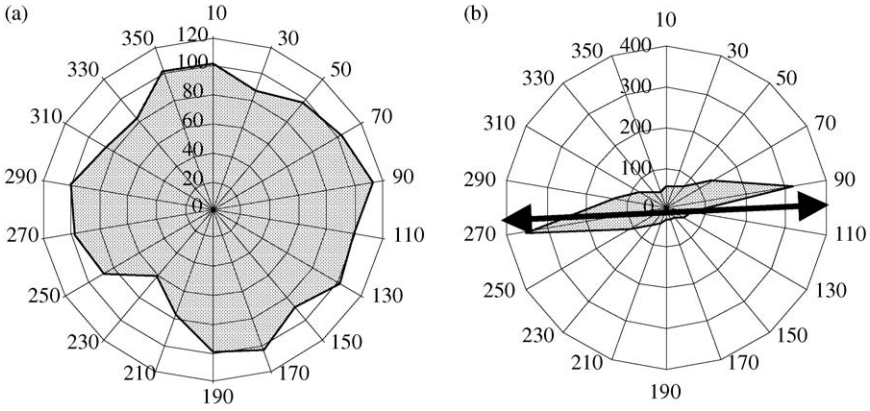

Figure 7 Effects of surface structure on cell migration angle. The possible migration angle range of 0–360° was subdivided into 18 ranges of 20°. Each migration angle value was allocated to one of these ranges and the occurrence was counted. In analogy to Fig. 4 the present diagrams show the frequency distribution of these occurrences on surfaces (a) and (b). The double arrow in the right figure represents the orientation of the grooves.

direction of the grooves. With the software used it was possible to estimate the correlation between migration direction and migration angle. The migration vector of several cells between two subsequent pictures had been calculated and expressed as a dot in the *XY*-diagram. Cells plated on the plane surface showed no correlation between migration distance and migration angle, i.e. the dots were evenly distributed in all directions (Fig. 6(a)). In contrast, cells which were seeded on the structured surface, migration distance and migration angle was directly correlated with the highest distance parallel to the grooves (Fig. 6(b)). As already noticed before, there were some cells, which switched from one groove into the neighbouring groove. These switching of the tracks can also be seen in the diagram of Fig. 6(b). Most dots can be found close the line $(x = 0)$. A few dots were found some micrometres away from that point and represent cells that switched grooves between two subsequent pictures.

The migration vector of each cell between two subsequent pictures is defined by the angle and size representing the migration distance. With the analysis software it was possible to determine these parameters separately. The diagram shown in Fig. 7(a) display the results of cells that were plated on the plane surface. The frequencies of the occurring migration angles were homogenously distributed within the 18 ranges of 20° in case of cells cultured on plane surfaces. However, when the cells were seeded on a grooved surface (surface B), the high frequencies were found in only two ranges: 80°–100° and in the opposite direction (170°–190°) (Fig. 7(b)).

The migration velocity pattern of the cells is shown in Fig. 8. No significant differences in the velocity frequencies were found between cells plated on the plane surface and cells plated on the grooved surfaces. The overall migration velocity on plane and grooved surfaces was also found to be similar (Fig. 8), although on grooved surfaces the velocity parallel to the grooves was increased in comparison perpendicular to the grooves (Fig. 6). These results are in contrast to those of Li *et al*. [15] investigating the migration of endothelial cells on unstructured and micro-patterned collagen matrices. They found that cells on micro-patterned matrices had the highest migration speed.

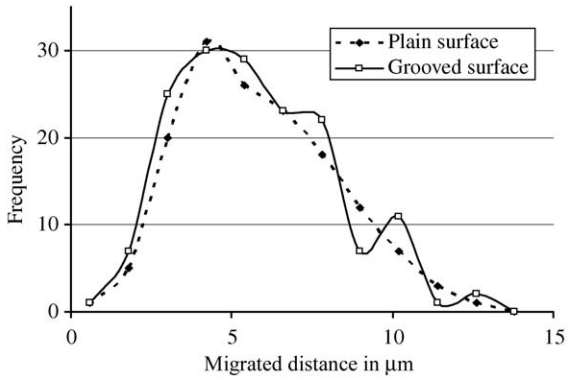

Figure 8 Migration velocity of the cells between two subsequent pictures was recorded for the cells plated on the plane surface and on the grooved surface. The average speed between two subsequent pictures was clustered into several speed ranges of velocities of 1.2 µm/15 min. In this figure the frequency pattern is presented.

The present study revealed that the present set-up based on fluorescent labelling of cells, long-term monitoring of cell shape and migration, using Confocal laser scanning microscope (CLSM), combined with a computer-assisted image analysis represents an easy but powerful tool to analyse cell–material interactions, taking trajectories, migration velocity distribution, migration orientation and cell shape (cell orientation) as indices.

Acknowledgments

We acknowledge the Swiss Technology-oriented program NANO 21 (TopNano21) for its financial support.

References

1. D. A. LAUFFENBURGER and A. HORWITZ, *Cell* **84** (1996) 359.
2. K. WEBB, V. HLADY and P. A. TRESCO, *J. Biomed. Mater. Res.* **49** (2000) 362.
3. A. CURTIS and C. WILKINSON, *Biochem. Soc. Symp.* **65** (1999) 15.
4. E. A. COX, D. BENNIN, A. T. DOAN, T. O'TOOLE and A. HUTTENLOCHER, *Mol. Biol. Cell* **14** (2003) 658.
5. B. WOJCIAK-STOTHARD, A. S. G. CURTIS, W. MONAGHAN, M. MCGRATH, I. SOMMER and C. D. W. WILKINSON, *Cell Motil. Cytoskeleton* **31** (1995) 147.

6. B. CHEHROUDI, T. R. GOULD and D. M. BRUNETTE, *J. Biomed. Mater. Res.* **23** (1989) 1067.
7. C. M. LO, H. B. WANG, M. DEMBO and Y. L. WANG, *Biophys. J.* **79** (2000) 144.
8. A. CURTIS, C. WILKINSON and B. WOJCIAK-STOTHARD, *Cell Eng. Inc. Mol. Eng.* **1** (1995) 35.
9. M. G. HONIG and R. I. HUME, *J. Cell Biol.* **103** (1986) 171.
10. P. K. HORAN, M. J. MELNICOFF, B. D. JENSEN and S. E. SLEZAK, *Meth. Cell Biol.* **33** (1990) 469.
11. A. BRUININK, in ''The Brain in Bits and Pieces'' (M. T. C. Verlag, Zollikon, CH) p. 23.
12. D. M. BRUNETTE, *Exp. Cell Res.* **167** (1986) 203.
13. E. T. DEN BRABER, J. E. DE RUIJTER, L. A. GINSEL, A. F. RECUM and J. A. JANSEN, *Biomaterials* **17** (1996) 2037.
14. A. CURTIS and P. CLARK, *Crit. Rev. Biocomp.* **5** (1990) 343.
15. S. LI, S. BHATIA, Y. L. HU, Y. T. SHIU, Y. S. LI, S. USAMI and S. CHIEN, *Biorheology* **8** (2001) 101.

Received 4 October
and accepted 10 October 2003